

Article

Energy Efficient Design of Massive MIMO Based on Closely Spaced Antennas: Mutual Coupling Effect

Peerapong Uthansakul * , Arfat Ahmad Khan , Monthippa Uthansakul and Pumin Duangmanee

School of Telecommunication Engineering, Suranaree University of Technology, Nakhon Ratchasimina 30000, Thailand; arfat_ahmad_khan@yahoo.com (A.A.K.); mtp@sut.ac.th (M.U.); puminsoft@gmail.com (P.D.)

* Correspondence: uthansakul@sut.ac.th; Tel.: +66-085-086-5588

Received: 10 July 2018; Accepted: 2 August 2018; Published: 5 August 2018



Abstract: Massive Multiple Input Multiple Output MIMO technology is a promising candidate for the next generation of communication applications, which essentially group hundreds of transmitting antennas together at the base station and provides the higher energy and spectral efficiency. In this article, the transmitting antennas are assumed to be closely spaced at the base station, which in turn results into a mutual coupling effect between the antenna terminals. The optimal system parameters and the energy efficiency are computed by considering the mutual coupling effect between the antenna terminals. Mutual coupling effect is deeply investigated on the energy efficiency and the other optimal parameters. We propose the domain splitter algorithm for the optimization of energy efficiency and the computation of different optimal system parameters in this article. The computational complexity of the proposed domain splitter algorithm is not dependent on the number of transceiver chains, and the detailed comparison is presented between the proposed and the reference algorithms on the basis of the computational complexity, which shows the effectiveness of the proposed domain splitter algorithm.

Keywords: power consumption; massive MIMO; power; time division duplex; mutual coupling; energy efficiency

1. Introduction

Wireless communication is the most vital and key technology in this modern era and with the ever-increasing trend of advances in the wireless technologies, a large number of users are using these technologies, which in turn require having a network with higher energy and spectral efficiency together with the simple signal processing [1–3]. Multiple Input Multiple Output (MIMO) systems have gained a lot of attraction, both in industry and academia, due to their ability to significantly improve the spectral efficiency, but the acquisition of higher spectral efficiency comes at the cost of complex computation and signal processing in the conventional MIMO systems [4]. Massive MIMO can significantly increase the performance of the system by just adopting the linear precoding and decoding schemes for the downlink transmission and the uplink reception due to the asymptotic orthogonality of the propagation channel, as compared to the conventional MIMO systems [5–8].

In Massive MIMO, hundreds of antennas have to be stationed on the top of a building or tower, serving a comparatively less number of users [9,10]. In the urban environment, the electromagnetic interaction between the antenna elements is inevitable due to the space limitations for the deployment of a large number of antenna elements at the base station, thereby, leads to a phenomena named Mutual Coupling [11]. In [12,13], the authors have investigated the mutual coupling effect on the performance of the conventional MIMO systems by calculating the closed-form expression of the channel capacity, based on closely spaced antenna elements. In [14], the authors have examined and investigated the

new challenges and issues regarding the deployment of hundreds of antenna elements at the Base Station (BS). In [15,16], the authors have modeled the channel and derived the closed-form expression of the channel by considering the effect of mutual coupling among the antenna terminals of Massive MIMO. The mutual coupling effect can be minimized by using the hardware-circuit calibration method and the signal-space calibration method [17–19]. The theory and benefits of the Massive MIMO are also applicable for the scenario of the wireless sensor networks where each sensor node can be taken as the user and the fusion center is equipped with large number of antennas, leading into the favorable propagation between the sensor nodes and the fusion center [20,21]. The initial focus of the researchers was on the spectral efficiency and the channel capacity of the communication devices, but the energy and power related pollution and the inevitable battery depletion of the wireless devices shifted the focus of the researchers to have more and more research on the green cellular networks in order to conserve as much energy as possible [2].

The energy efficiency is significantly dependent on the number of transceiver chains, transmitted and the consumed power [22,23]. The power consumption of the conventional MIMO systems is always taken as a fixed quantity due to the limited number of transmitter chains [24]. However, this assumption is not valid for the Massive MIMO, because the circuit power consumption is significantly dependent on the number of transmitter chains. The number of transceiver chains required for the system can be reduced by using the hybrid analogue to digital transceivers. In [25], the authors evaluate the performance of hybrid analogue to digital precoders by modelling the power consumptions of the RF chains. Motivated by the above research [25], the authors in [26,27] work on the energy efficient designing of the hybrid analogue to digital transceivers for the single carrier in [26] and for the single and multi-carrier large antenna arrays in [27] for the perfect channel conditions. In [28], the authors have investigated the energy and spectral efficiency of Massive MIMO at different channel situations and showed that the large number of antenna elements at the base station can significantly enhance the energy efficiency with orders of magnitude compared to the conventional MIMO systems, but, they fixed the total power consumption of the circuit, which in turn let them have an unbounded energy efficiency. In [29], the authors have investigated the energy efficiency and calculated the capacity limits of Massive MIMO, but the authors have not modelled the power consumption of the circuit in a correct way. They have not taken the power consumption during the decoding and coding, channel estimation and the linear processing, which in turn let them have the substantial enhancement in the energy efficiency. In [30–32], the authors have investigated the tendency of the energy efficiency with respect to the increase in the number of transmitting antennas, users and the transmitted power, and showed that the energy efficiency depicts the response of quasi concave function in terms of the number of transmitting antennas in [30], and in terms of the number of users and the transmitted power in [31,32] respectively, by using the refined and appropriate model of the total circuit power consumption. Motivated by the above researches [30–32], the authors in [33] extended the results under different channel conditions, by using the refined and correct model of the total circuit power consumption.

In the corpus of the researches [22–33], the authors have optimized and investigated the energy efficiency along with the computation of different optimal system parameters, by taking the assumption that the transmitting antennas at the BS are spaced enough, in order to nullify the effect of mutual coupling among the antenna elements. This assumption is not correct for the massive MIMO wireless communication systems, especially under the scenario of the urban environment, due to the space limitations for the deployment of a large number of antenna elements at the base station. Therefore, the effect of mutual coupling is inevitable among the antenna elements for Massive MIMO wireless communication systems. In [34], the authors have optimized the energy efficiency and computed the optimal transmitting antennas and users by considering the effect of mutual coupling between the antenna elements at the BS under the perfect channel situation.

In this article, we have derived and formulated the mathematical expressions of the achievable spectral efficiency along with the energy efficiency by taking the effect of mutual coupling between the transmitting antennas at the base station with respect to the different channel conditions. We

have designed the energy efficient Massive MIMO by using the correct model of the circuit power consumption and computed the number of optimal user terminals, transmitting antennas and the corresponding consumed as well as the transmitted power. Mutual coupling effect among the antenna elements have been thoroughly investigated on the energy efficiency and other optimal parameters, by varying the length of the transmitting antennas and the spacing between them. The optimization problem of energy efficiency has been formulated in order to calculate the optimal parameters with respect to the different channel conditions. We have proposal a domain splitter algorithm for the optimization of energy efficiency, and calculation of the optimal parameters. A detailed comparison is presented between the reference and the proposed algorithms in terms of the computation complexity. At the end, we have made simulations in order to support and show the effectiveness of the mathematical modelling, where the simulation result shows the optimally achieving energy efficiency and other optimal system parameters, with respect to different channel conditions and the spacing between the antenna elements.

This article is further arranged as follows. First, we have modelled the channel and derived the spectral efficiency of the Massive MIMO, by taking the effect of mutual coupling among the antenna elements, with respect to the different channel situations in Section 2. Next, we have modelled the circuit power consumption of massive MIMO in Section 3. Furthermore, we have formulated the optimization problem of energy efficiency in Section 4. In Section 5, the domain splitter algorithm and the complexity comparison are presented between the proposed and the reference algorithms. The simulation results are provided in Section 6. Section 7 belongs to the conclusion where we summarize and conclude all the discussions.

The notation used in this paper is as follows: $(\cdot)^{-1}$, $Ci(\cdot)$, $(\cdot)^T$, $Si(\cdot)$, $(\cdot)^*$ and $(\cdot)^H$ denotes the inverse, cosine integral, transpose, sine integral, conjugate, and the Hermitian operator respectively, $E[\cdot]$, $\|\cdot\|^2$ denotes the expectation and the norm operation, Z_+ denotes the positive integers, $\log_2(x)$ and $\ln(x)$ denotes the logarithm of x with respect to base 2 and e , $(\cdot)'$, $(\cdot)''$ denotes the first order derivative and the second order derivatives, \sim , $var(\cdot)$ denotes the approximation and the variance notation, $CN(x, y)$ denotes the complex normal distribution with mean x and the variance y . Additionally, $trace(\cdot)$ represents the matrix trace operation.

2. Channel Modelling and the Spectral Efficiency

In Massive MIMO, hundreds of antennas have to be stationed on the top of a building or tower, serving comparatively small number of users. Time Division Duplex is the most desirable scheme in the case of Massive MIMO, because of the reciprocity between the uplink and downlink channels during each coherence block, as compared to Frequency Division Duplex (FDD), where pilot overhead in each coherence block is dependent on the number of transmitting antennas at the BS. In FDD, we have to use different frequencies in the uplink and downlink and the pilot overhead of the channel estimation is proportional to the number of transmitting antennas, leading to a very challenging situation at the user terminals to acquire the downlink channel state information and then feedback the acquired channel state information to the base station. The Massive MIMO was basically imagined for TDD protocol, but can be applied also in FDD by using the various techniques. Figure 1 unveils the frame sequence in the case of TDD protocol, the Channel State Information C.S.I at the BS can be estimated with the help of Uplink training signals or pilots for T_p^{ul} channel uses and the estimated C.S.I can be exploited during the downlink transmission for T_p^{dl} channel uses. The performance of the massive MIMO relies critically on the correctness of the C.S.I during each coherence block U .

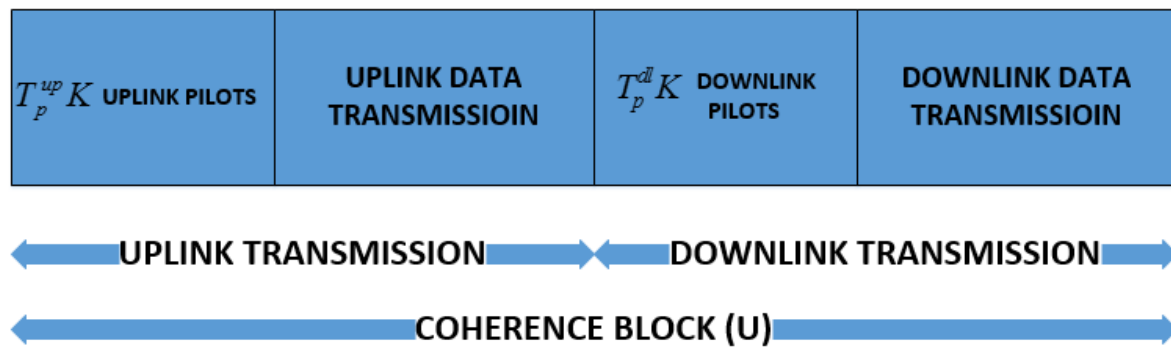


Figure 1. Frame Structure of Massive MIMO.

Consider the M number of the dipole antennas are equipped at the BS, having the length L and separated by a distance s , serving K number of uniformly distributed single antenna users as can be seen in Figure 2. Therefore, the received signal at the base station can be written as:

$$y = \sqrt{p}Gx + n \tag{1}$$

where $x = [x_1, x_2, \dots, x_K]$ is the matrix of the transmitted signals from the K number of uniformly distributed single antenna users and y is the received signal matrix with the dimension of $M \times 1$ at the base station. p can be deemed as the average transmitted power and n is the Additive White Gaussian Noise with the dimension of $M \times 1$ and has the zero mean and unity variance, whereas G is the channel matrix with the dimension of $M \times K$.

Massive MIMO can enhance the performance by exploiting the orthogonality between the channels of the desired and the interference signals, which in turn results into the communication reliability, by using the linear signal processing during the uplink transmission and the downlink reception. Thus, the linear precoding matrix V can be written as:

$$V = \begin{cases} G^* \text{ MRT} \\ G(G^H G)^{-1} \text{ ZF} \\ G\left(G^H G + \frac{K}{p}\right)^{-1} \text{ MMSE} \end{cases}$$

As explained earlier, the transmitting antennas at the base station are closely spaced, leading into the effect of mutual coupling. Thus, the channel matrix by considering the mutual coupling effect among the base station antennas can be expressed as:

$$G = CHD^{1/2}$$

where C is the mutual coupling matrix with the dimension of $M \times M$ and H is the Rayleigh small scale fading matrix. D is a $K \times K$ large scale diagonal matrix and can be written as:

$$D = \text{diag}(\beta_1 \dots \dots \beta_K)$$

where β_k shows the path loss or the large scale fading between the base station and the k th user terminal. The mutual coupling matrix when the M number of the dipole antennas are equipped at the BS can be written as [13]:

$$C = (z_L + z_s)(z_L I_M + z_c)^{-1} \tag{2}$$

where z_L and z_s represent the load and the self-impedance respectively. z_c represents the matrix of mutual impedance, where the diagonal entries showing the self-impedances of the transmitting

antennas, and, the non-diagonal entries are showing the mutual impedances. The mutual impedance between two particular transmitting dipole antennas i and j can be written as [35]:

$$z_{ij} = \begin{cases} 30[0.577 + \ln(2\pi) - Ci(2\pi) + j Si(2\pi)] & i = j \\ 30 \begin{bmatrix} [2Ci(\beta s) - Ci(\beta\mu_1) - Ci(\beta\mu_2)] + \\ -30j[2Si(\beta s) - Si(\beta\mu_1) - Si(\beta\mu_2)] \end{bmatrix} & i \neq j \end{cases} \quad (3)$$

where:

$$\begin{aligned} \mu_1 &= \sqrt{s^2 + L^2} + L \\ \mu_2 &= \sqrt{s^2 + L^2} - L \\ \beta &= \frac{2\pi}{\lambda} \end{aligned}$$

where s is the distance between two antenna terminals and L is the length of the dipole antenna element as shown in Figure 2. Ci , Si represent the cosine and sine integrals respectively and can be written as:

$$\begin{aligned} Ci(s) &= \int_{-\infty}^s \frac{\cos(s)}{s} ds \\ Si(s) &= \int_{-\infty}^s \frac{\sin(s)}{s} ds \end{aligned}$$

Assume that, the zero forcing linear detection scheme is implemented at the base station, then, the signal received at the base station can be expressed as:

$$y = V^H(\sqrt{p}Gx + n)$$

Similarly, the signal received from the k th user terminal can be written as:

$$\begin{aligned} y_k &= V_k^H(\sqrt{p}Gx_k + n) \\ y_k &= \sqrt{p}x_k + v_k^H n \end{aligned}$$

where v_k represent the k th column of the detection matrix V and the equivalent noise $v_k^H n$ can be expressed as: $v_k^H n \sim \text{CN}(0, \|v_k^H\|^2)$. The Signal to Noise Ratio (S.N.R) at the corresponding k th link can be expressed as:

$$SNR_k = \frac{p}{\|V_k^H\|^2} \quad (4)$$

As we know $\|V\|^2 = VV^H$. Thus, the above equation can be written as:

$$SNR_k = \frac{p}{(G_k^H G_k)^{-1}} \quad (5)$$

The corresponding achievable rate can be illustrated as:

$$R_k = \text{E} \left[\log_2 \left(1 + \frac{p}{(G_k^H G_k)^{-1}} \right) \right] \quad (6)$$

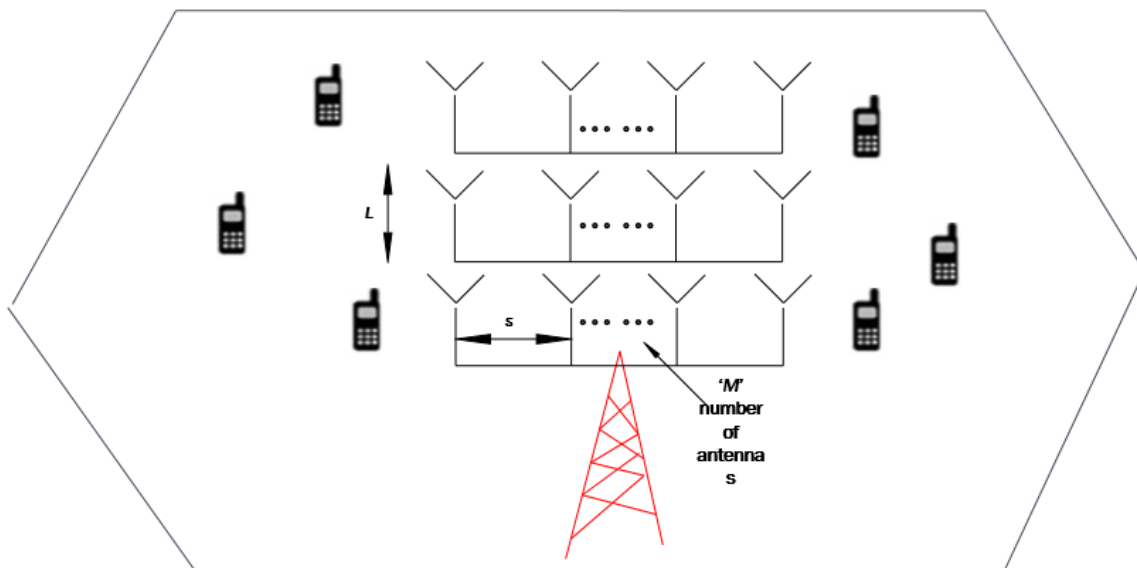


Figure 2. Massive MIMO with M antenna terminals.

Theorem 1. In Rayleigh fading channel, when $M \geq K + 1$ and ZF detector is implemented at the base station, then, the achievable rate for the k th user terminal can be written as:

$$R_k = \frac{1}{\ln(2)} \ln \left(1 + p\beta_k \text{trace} \left(C^H C \right) \times (M - K) \right) \tag{7}$$

Proof of the Theorem 1. See Appendix A. □

The overall spectral efficiency (R_K) for the total K number of users can be written as:

$$R_K = B \sum_{k=1}^K R_k \tag{8}$$

Put the value of R_k from (7) to (8):

$$R_K = \frac{B}{\ln(2)} \sum_{k=1}^K \ln \left(1 + p\beta_k \text{trace} \left(C^H C \right) \times (M - K) \right)$$

$$R_K = K \frac{B}{\ln(2)} \ln \left(1 + p\beta_k \text{trace} \left(C^H C \right) \times (M - K) \right)$$

The overall spectral efficiency by taking the overhead of the training signals into account can be written as:

$$R_K = K \left(1 - \frac{TK}{U} \right) \frac{B}{\ln(2)} \ln \left(1 + \left(p\beta_k \text{trace} \left(C^H C \right) \times (M - K) \right) \right) \tag{9}$$

Whereas, T is the total length of the relative pilot sequence.

Computation of the Spectral Efficiency under the Scenario of Imperfect Channel Situation

The performance of the Massive MIMO is significantly dependent on the acquisition of the C.S.I. However, having a perfect (C.S.I) is almost unfeasible in terms of real-world scenario, which in turn leads to interference among the user terminals. During the uplink transmission, the C.S.I is computed by using the pilot signals, and, let the uplink power of the pilot signal for the k th user terminal be

$\left(\frac{\sigma^2 p}{\beta_k}\right)$ and the total length of the orthogonal pilot signals be $T_p^{ul} K$ as shown in Figure 1. The estimated channel matrix \hat{G} can be expressed as:

$$\hat{G} = G + \varepsilon$$

where ε is the channel estimation error during the acquisition of the frequency response of propagation channel. Therefore, the signal received at the BS can be written as:

$$y_{lm} = V^H(\sqrt{p}Gx + \varepsilon + n)$$

Theorem 2. In Rayleigh fading channel, when $M \geq K + 1$ and ZF detector is implemented at the BS, then, the achievable rate for the k th user terminal by computing the estimated channel with the help of the MMSE estimator for the imperfect channel condition can be expressed as:

$$R_{k,lm} = \log_2 \left(1 + \frac{p\beta_k \text{trace}(C^H C) \times (M - K)}{1 + \frac{1}{T_p^{ul}} + \frac{1}{pKT_p^{ul}}} \right) \quad (10)$$

Proof of Theorem 2. See Appendix B. \square

Similarly, the overall spectral efficiency by taking the overhead of the training signals into account for the imperfect channel conditions can be expressed as:

$$R_{K,lm} = K \left(1 - \frac{TK}{U} \right) \frac{B}{\ln(2)} \ln \left(1 + \frac{p\beta_k \text{trace}(C^H C) \times (M - K)}{1 + \frac{1}{T_p^{ul}} + \frac{1}{pKT_p^{ul}}} \right) \quad (11)$$

3. Power Consumptions

Total power consumption can be expressed as an additive summation of the overall circuit power consumption, and the transmitted or power amplifier power. We have modeled the total circuit power consumption as well as the transmitted power in this section. The total transmitted power P_t can be expressed as:

$$P_t = \frac{B\alpha^2}{\eta} \sum_{k=1}^K p_k \quad (12)$$

where η is the efficiency of the PA's and $B\alpha^2$ is the overall noise power. Assume that the users are distributed uniformly in between the minimum d_{min} and the maximum distance d_{max} , then, the total transmitted power by using the uniform distribution can be expressed as:

$$P_t = \frac{B\alpha^2 K p}{\eta} \left(\frac{d_{max}^{\alpha+2} - d_{min}^{\alpha-2}}{(1 + \frac{\alpha}{2})d_{max}^2 - d_{min}^2} \right) \quad (13)$$

where α represent the path loss factor and the circuit power consumption can be written as the power consumed in the transceiver chains (P_{TRC}) (filters, convertors and the mixers powers), power consumption during the site cooling and maintenance P_{fx} , coding and the decoding power $P_{cod/doc}$, linear processing power $P_{L.P}$, power consumed during the estimation of the channel P_{es} and the oscillator power P_o . Thus, the total power consumption can be expressed as:

$$P_c = P_{fx} + P_{TRC} + P_o + P_{cod/doc} + P_{L.P} + P_{es} \quad (14)$$

The consumed power in the transceiver chains P_{TRC} can be written as:

$$P_{TRC} = M(P_T) + K(P_R) \quad (15)$$

where P_T, P_R represent the consumption of power at the transmitter and the user end. The power consumed during the decoding and coding of the signals is dependent on the number of bits, so, the power consumed during this process can be written as:

$$P_{cod/doc} = R_K(P_{cod} + P_{doc}) \quad (16)$$

where P_{doc}, P_{cod} is the power consumption during the process of decoding and coding of the received and the transmitted signals. As explained earlier, massive MIMO relies significantly on the accurate acquisition of the frequency response, so, the timely acquisition of the frequency response is of timely important, and the consumed power during the channel estimation P_{es} can be expressed as [34]:

$$P_{es} = \frac{2K^2T^{ul}B}{U} \left[\frac{M}{\eta_{Bs}} + \frac{2}{\eta_{ue}} \right] \quad (17)$$

where $\frac{B}{U}$ represent the number of coherence blocks per second, η_{Bs}, η_{ue} is the computational efficiencies at the base station and the user end during the estimation of the channel. The power consumption during the linear processing $P_{L.P}$ can be interpreted as [36]:

$$P_{L.P} = \frac{B}{U} \left(\frac{K^3}{3\eta_{Bs}} + \frac{MK(3K+1)}{\eta_{Bs}} \right) \quad (18)$$

Thus, the overall power consumption P_{tot} by using the (13)–(18) can be written as:

$$\begin{aligned} P_{tot} &= P_t + P_{fx} + P_{TRC} + P_o + P_{cod/doc} + P_{L.P} + P_{es} \\ P_{tot} &= P_{fx} + \frac{B\alpha^2Kp}{\eta} \left(\frac{d_{max}^{\alpha+2} - d_{min}^{\alpha-2}}{(1+\frac{\alpha}{2})d_{max}^2 - d_{min}^2} \right) + M(P_T) + K(P_R) + R_K(P_{cod} + P_{doc}) \\ &+ \frac{2K^2T^{ul}B}{U} \left[\frac{M}{\eta_{Bs}} + \frac{2}{\eta_{ue}} \right] + \frac{B}{U} \left(\frac{K^3}{3\eta_{Bs}} + \frac{MK(3K+1)}{\eta_{Bs}} \right) \end{aligned} \quad (19)$$

Let:

$$\begin{aligned} \delta_x &= \left(\frac{d_{max}^{\alpha+2} - d_{min}^{\alpha-2}}{(1+\frac{\alpha}{2})d_{max}^2 - d_{min}^2} \right), C_o = P_{fx} + P_o, C_1 = P_R, C_2 = \frac{B}{U} \left(\frac{4T^{ul}}{\eta_{ue}} \right), C_3 = \frac{B}{U} \left(\frac{1}{3\eta_{Bs}} \right), \\ D_o &= P_T, D_1 = \frac{B}{U} \left(\frac{1}{\eta_{Bs}} \right), D_2 = \frac{B}{U} \left(\frac{3}{\eta_{Bs}} + \frac{2T^{ul}}{\eta_{Bs}} \right) \end{aligned}$$

Thus, the total power consumption (19) by using the above given substitutions can be expressed as:

$$P_{tot} = \frac{B\alpha^2KpS_x}{\eta} + \sum_{i=0}^3 C_i K^i + M \sum_{j=0}^2 D_j K^j \quad (20)$$

4. Problem Definition

In this section, we have formulated the problem and derived the mathematical expressions of the energy efficiency for the perfect and imperfect channel situation. Energy efficiency can be expressed as the ratio of total spectral efficiency and the total power consumption i.e.,

$$EE = \frac{R_K}{P_{tot}}$$

Thus, the Energy efficiency of Massive MIMO $EE_P(M, K, p)$ by using the (9) and (20) under the perfect channel condition can be expressed as:

$$EE_P(M, K, p) = \frac{K \left(1 - \frac{TK}{U}\right) \frac{B}{\ln(2)} \times \ln(1 + p\beta_k \text{trace}(C^H C) \times (M - K))}{\frac{Ba^2 K p S_x}{\eta} + \sum_{i=0}^3 C_i K^i + M \sum_{j=0}^2 D_j K^j} \tag{21}$$

Energy efficiency needs to be optimized, so, the optimization problem of Energy efficiency can be formulated as:

$$\begin{aligned} & \text{Max} && EE_P(M, K, p) \\ & \text{Subject to} && M \in +, K \in + \\ & && K < M, p > 0 \end{aligned} \tag{22}$$

Similarly, the energy efficiency of Massive MIMO $EE_{Im,P}(M, K, p)$ by using the (11) and (20) along with the optimization problem for the Imperfect channel condition can be expressed as:

$$EE_{Im,P}(M, K, p) = \frac{K \left(1 - \frac{TK}{U}\right) \frac{B}{\ln(2)} \times \ln \left(1 + \frac{p\beta_k \text{trace}(C^H C) \times (M - K)}{1 + \frac{1}{T_p^u} + \frac{1}{pKT_p^u}}\right)}{\frac{Ba^2 K p S_x}{\eta} + \sum_{i=0}^3 C_i K^i + M \sum_{j=0}^2 D_j K^j} \tag{23}$$

$$\begin{aligned} & \text{Max} && EE_{Im,P}(M, K, p) \\ & \text{Subject to} && M \in +, K \in + \\ & && K < M, p > 0 \end{aligned} \tag{24}$$

We need to calculate the optimal number of BS antennas, users, and their corresponding transmitted power and energy efficiency. The M, K and p are closely associated and related to each other as it can be seen in the (21) and (23). Take the following substitutions and their corresponding interpretations (Table 1) into account for the simplification of $EE_P(M, K, p)$ and $EE_{Im,P}(M, K, p)$.

Table 1. Substitutions and physical interpretations.

Substitution	Interpretation
$r_1 = K$	Number of optimal user terminals.
$r_2 = M/K$	Number of optimal active antennas per user terminal.
$r_3 = pK$	Total transmitted power.

Following the above mentioned substitutions, the $EE_P(M, K, p)$ and $EE_{Im,P}(M, K, p)$ can be modified as:

$$EE_P(r_1, r_2, r_3) = \frac{r_1 \left(1 - \frac{Tr_1}{U}\right) \frac{B}{\ln(2)} \times \ln(1 + r_1 \beta_k \text{trace}(C^H C) \times (r_2 - 1))}{\frac{Ba^2 r_3 S_x}{\eta} + \sum_{i=0}^3 C_i r_1^i + r_2 \sum_{j=0}^2 D_j r_1^{j+1}} \tag{25}$$

$$EE_{Im,P}(r_1, r_2, r_3) = \frac{r_1 \left(1 - \frac{Tr_1}{U}\right) \frac{B}{\ln(2)} \times \ln \left(1 + \frac{r_3 \beta_k \text{trace}(C^H C) \times (r_2 - 1)}{1 + \frac{1}{T_p^u} + \frac{1}{r_3 T_p^u}}\right)}{\frac{Ba^2 r_3 S_x}{\eta} + \sum_{i=0}^3 C_i r_1^i + r_2 \sum_{j=0}^2 D_j r_1^{j+1}} \tag{26}$$

Thus, the corresponding mathematical optimization problems for the perfect and imperfect channel situation can be simplified as:

$$\begin{aligned} & \text{Max} && EE_P(r_1, r_2, r_3) \\ & \text{Subject to} && r_1 \in +, r_2 \in + \\ & && r_3 > 0 \end{aligned} \quad (27)$$

And:

$$\begin{aligned} & \text{Max} && EE_{Im,P}(r_1, r_2, r_3) \\ & \text{Subject to} && r_1 \in +, r_2 \in + \\ & && r_3 > 0 \end{aligned} \quad (28)$$

5. Computation of the Optimal Parameters and the Complexity Comparison

In this section, we have proposed and discussed the domain splitter algorithm to calculate the optimal parameters and the comparison is presented between the proposed and the reference algorithms, in terms of the computation complexity. We have named the proposed algorithm as the domain splitter algorithm because the proposed algorithm splits the domains of $EE_P(r_1, r_2, r_3)$ and $EE_{Im,P}(r_1, r_2, r_3)$, and then find the solution in each respective domain as shown in Figure 3. The $EE_P(r)$ and $EE_{Im,P}(r)$ shows the response of the quasi concave and depicts the one and the only one zero crossing at the points $EE'_P(r) = 0$ and $EE'_{Im,P}(r) = 0$ in each respective domain $r = (r_1, r_2, r_3)$, as per the Appendixes C and D. In the Appendixes C and D, the solution of the energy efficiency is derived in each respective domain $r = (r_1, r_2, r_3)$ and the optimal values are computed at the points $EE'_P(r) = 0$ and $EE'_{Im,P}(r) = 0$ by using these solutions. The Figure 3 shows the domain splitter algorithm and the simulation methodology where the optimal values of $r = (r_1, r_2, r_3)$ are computed until the convergence. Finally, the acquired optimal values are used to compute the number of optimal user terminal, optimal transmitters along with the transmitted power, energy and the spectral efficiency.

Table 2 shows the computation complexity between the proposed and the reference schemes and $W(n)$ is the lambert omega operation. It can be seen from Table 2 that the computational complexity of the reference algorithms is dependent on the multiplication of the number of transmitting antennas at the BS with the number of user terminals ($M \times K$). As Massive MIMO is dependent on the theory of large numbers of transmitting antennas at the BS, so, the computational complexity behind the reference algorithms is so high. The proposed algorithm (domain splitter algorithm) significantly improves the computation complexity where the energy efficiency gets saturated at the third iteration as shown in Figure 12.

Table 2. Complexity Comparison.

Algorithm	Computational Complexity
Reference [32] algorithm.	$M \times K \left(\left(2^{W(n)} \right) \right)$
Reference [34] algorithm.	$M \times K \left(\left(n^2 2^{W(n)} \right) \right)$
Reference [37] Algorithm	$M \times K \left(\left(2^{W(n^2)} \right) \right)$
Proposed Algorithm	$3 \left(\left(n^3 \ln(n^3) \right) \right)$

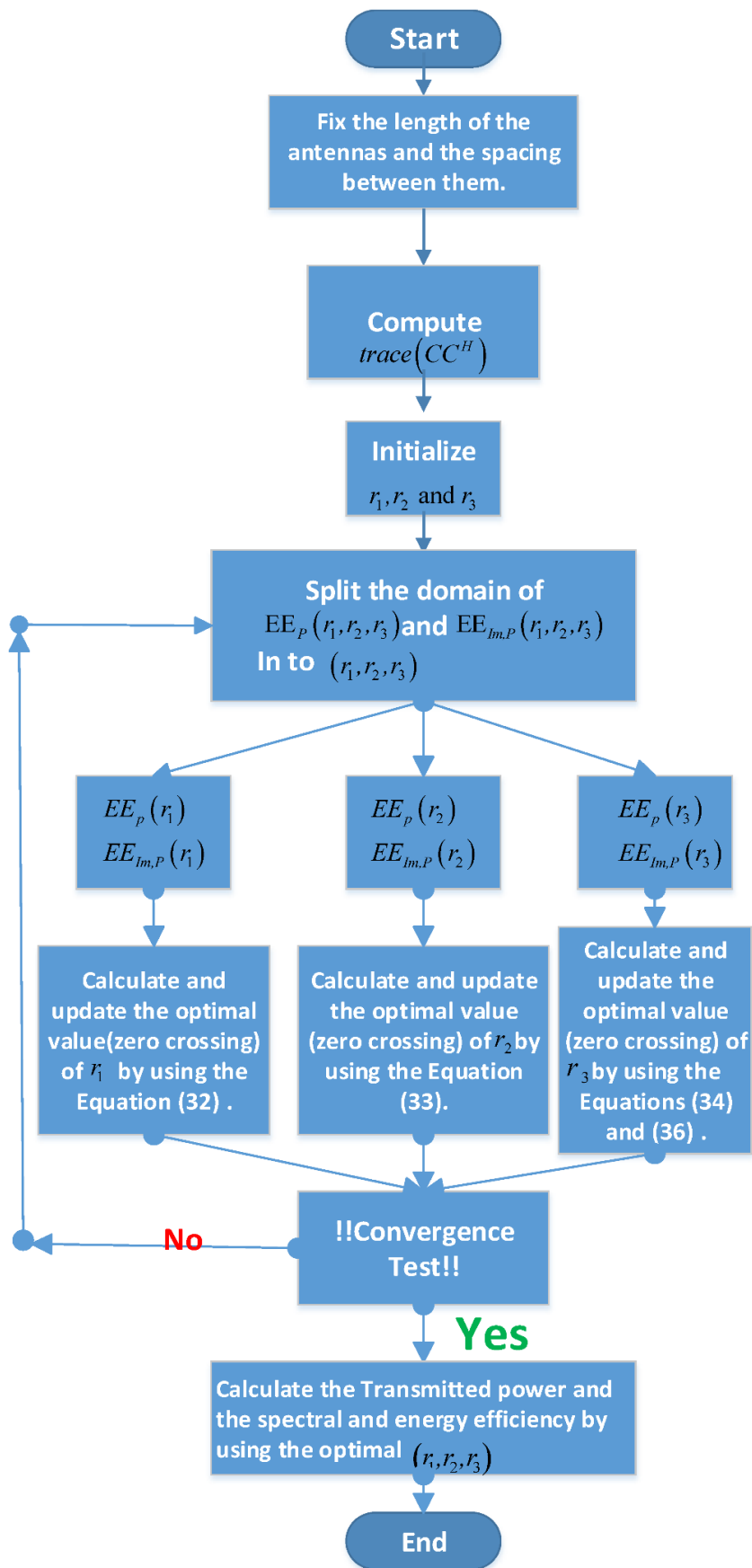


Figure 3. Domain Splitter Algorithm.

6. Simulations

We have performed simulations in order to test and demonstrate the effectiveness of the domain splitter algorithm along with computation of different optimal system parameters. Table 3 unveils the basic simulation parameters used for the simulations. We have used the acronyms of PCSI and ICSI for the perfect and imperfect channel state information respectively in the simulation figures. Figure 4 unveils the input impedances by varying the length of the antenna, where the real part of the antenna impedance is showing the power that is either absorbed or radiated away and the imaginary part is showing the stored power. Input impedance depends significantly on the length of the antenna terminal, as it can be seen from Figure 4. Figure 5 unveils the mutual impedance between the antenna terminals with respect to the spacing among the antennas, calculated by using the (3), at different lengths of the antenna terminal.

Table 3. Simulation Parameters.

Parameter	Value
Coherence Block Interval U	1800
Path loss exponent α	3.8 (Urban environment)
Computational efficiency at Base station (η_{Bs})	12 Gflops/W
Computational efficiency at the user end (η_{ue})	5.5 Gflops/W
Minimum distance d_{min}	30 m
Pilot lengths (T_p^{ul} , T)	1, 2
PA efficiency (η)	35%

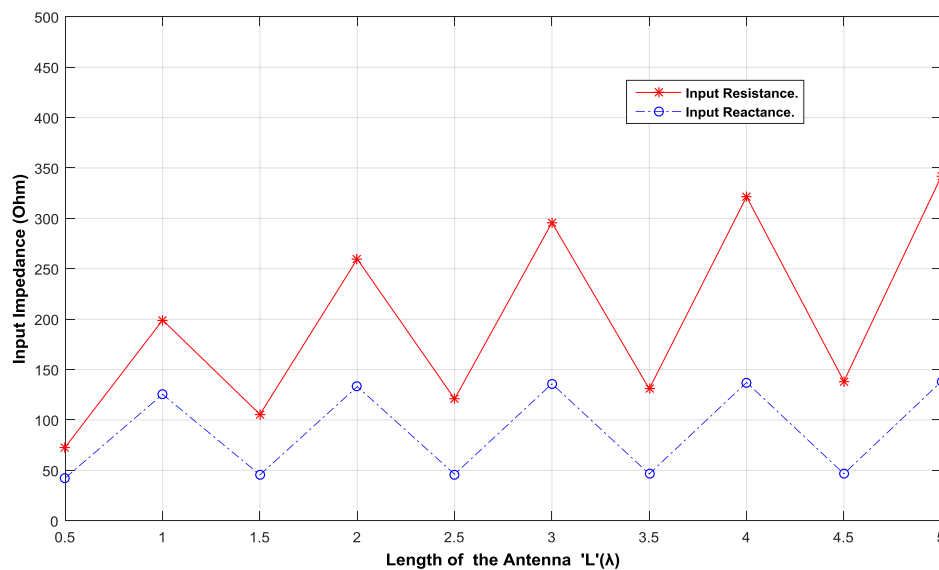


Figure 4. Input Impedance.

Figure 6 unveils the total number of optimal BS antennas with respect to the maximum distance between the base station and the users, at different circuit power consumption and at different spacing among the BS antennas. When the BS antennas are closely spaced, then it leads to mutual coupling and a higher number of the transmitting antennas are required. The effect of the mutual coupling and different antenna spacing on the optimal number of transmitters under the different channel situations can be seen in Figure 6.

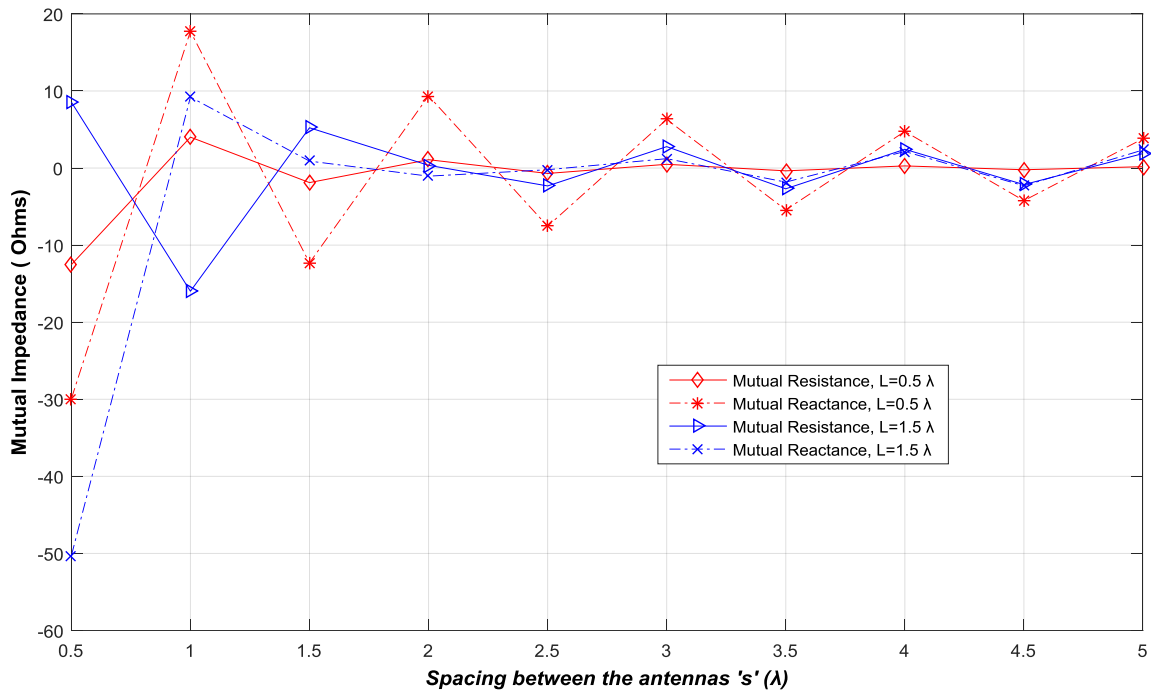


Figure 5. Mutual Impedances at different inter-antenna spacing.

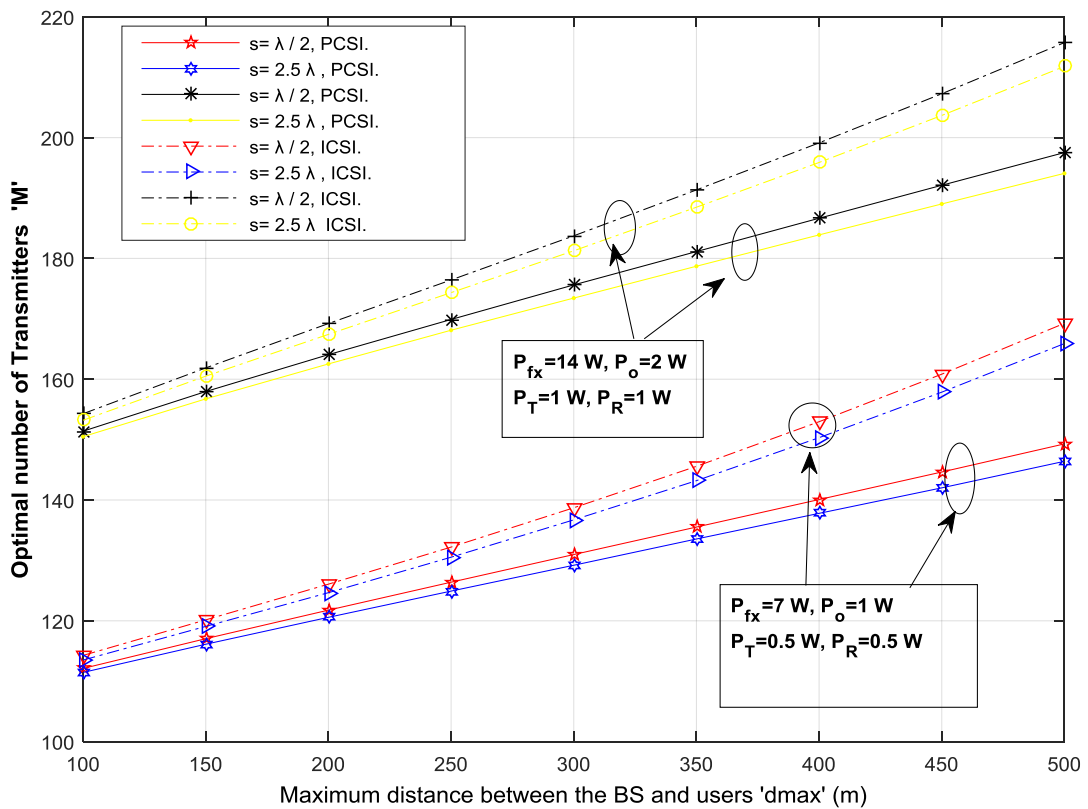


Figure 6. Number of optimal Transmitters.

When the maximum distance between the base station and the end users gets increased, then, the number of optimal BS antennas required for the system will be increased, in order to cover more distance as shown in Figure 6. Similarly, Figure 7 shows the optimal number of user terminals with

respect to the maximum distances (100–500 m) between the BS and the users, at different circuit power consumption and at different spacing among the BS antennas. More transmitted power is required when the BS antennas are closely spaced to overcome the mutual coupling effect along with the imperfect channel conditions as shown in Figure 8. Furthermore, high circuit power consumption leads to have more transmitted power to accommodate the higher number of BS antennas and the end users, and it is significantly dependent on the maximum distance between the BS and the users as shown in Figures 8 and 9. Figure 10 unveils the effect of mutual coupling on the achievable spectral efficiency of the system, and when the BS antennas are more closely spaced, then, the overall spectral efficiency gets reduced. As the system requires to have more transmitted power when the maximum distances between the BS and users gets increased, thereby, leads to have the reduction in the overall spectral efficiency of the system as shown in Figure 10.

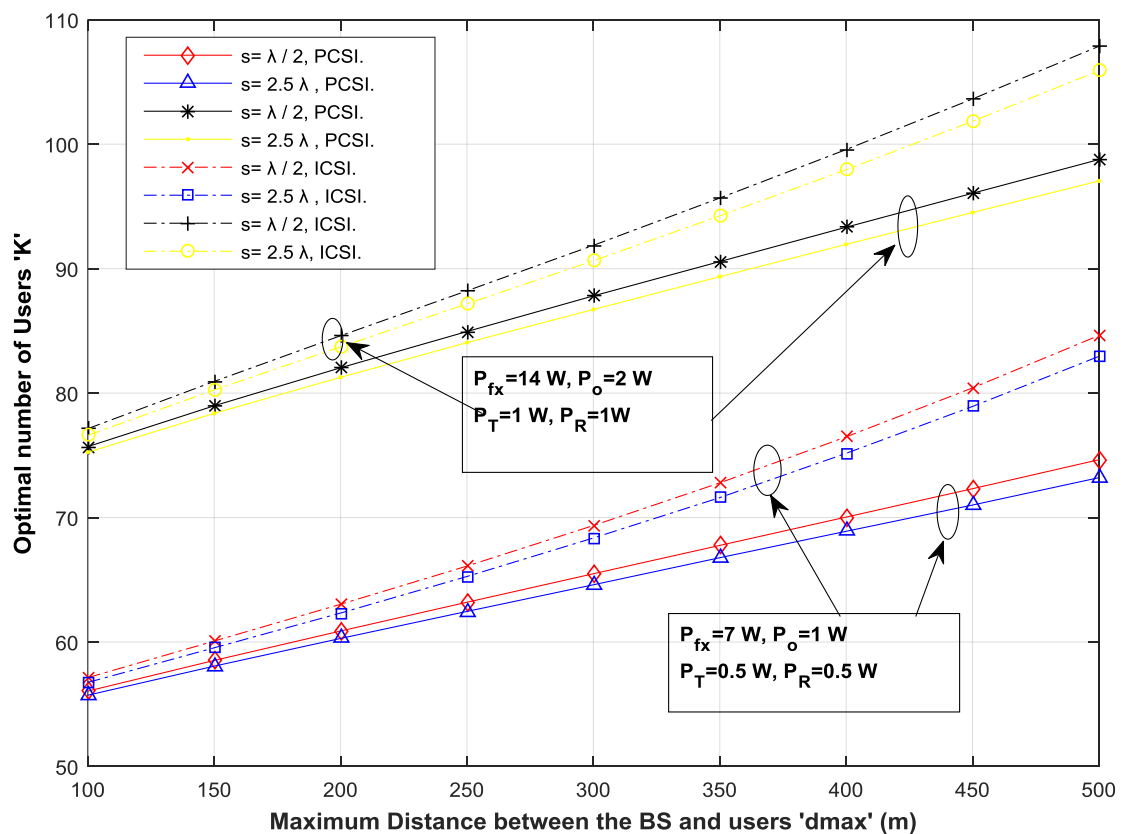


Figure 7. Number of optimal Users.

Similarly, Figure 11 unveils the mutual coupling effect on the overall energy efficiency of the system with respect to the different maximum distances between the BS and the end users, and imperfect channel situation leads to have a reduction in the overall achievable energy efficiency, due to the higher consumed as well as the transmitted power. Figure 12 unveils the computational complexity and the convergence of the proposed domain splitter algorithm, where the convergence of the energy efficiency can be examined with respect to the number of iterations. The energy efficiency goes into the saturation at the 3rd iteration, so, the computational complexity of the domain splitter algorithm in terms of Landau’s big O notation can be written as: $3((n^3 \ln(n^3)))$. A detailed comparison between the proposed and the reference algorithms in terms of computation complexity has been presented and discussed in Table 3.

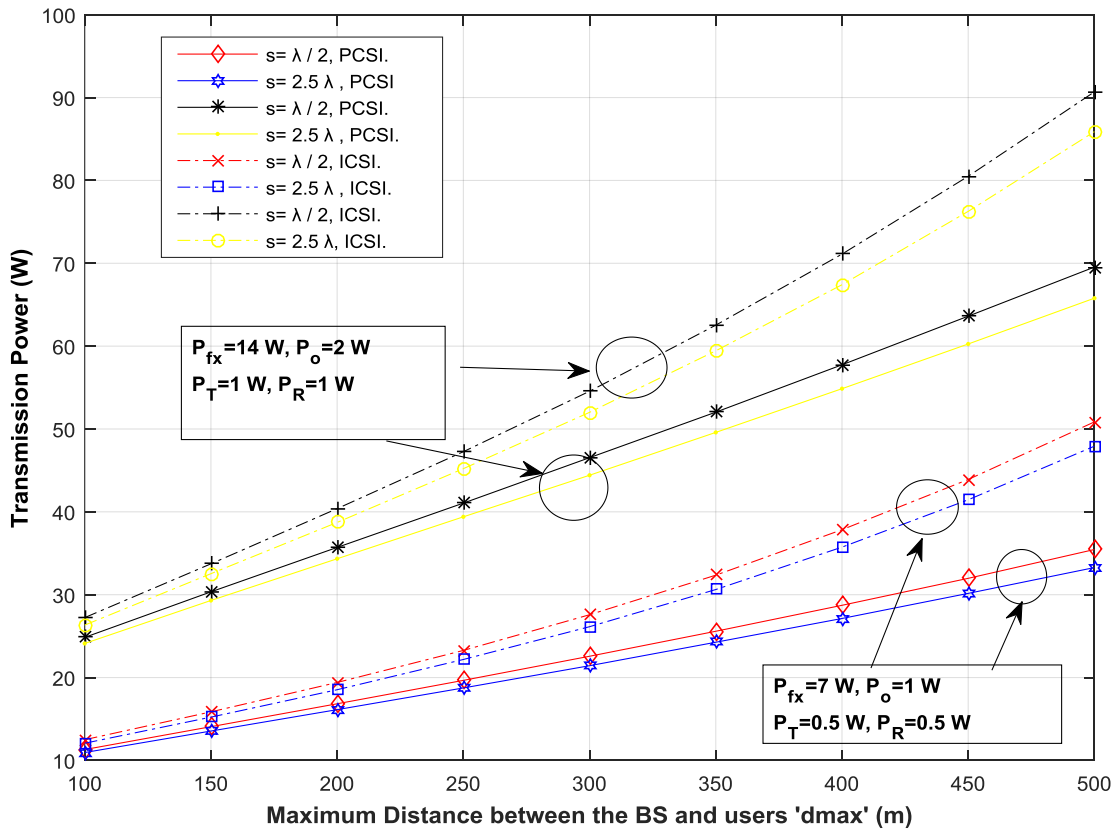


Figure 8. Transmission Power.

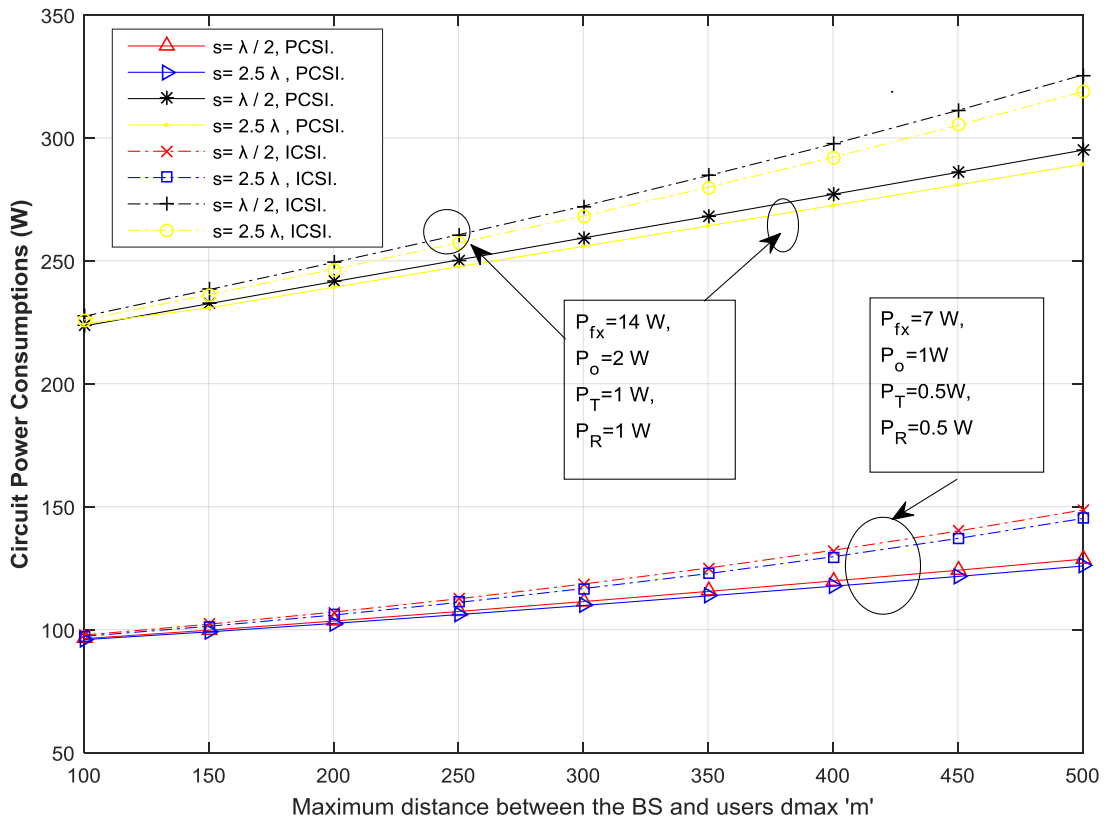


Figure 9. Circuit Power Consumption.

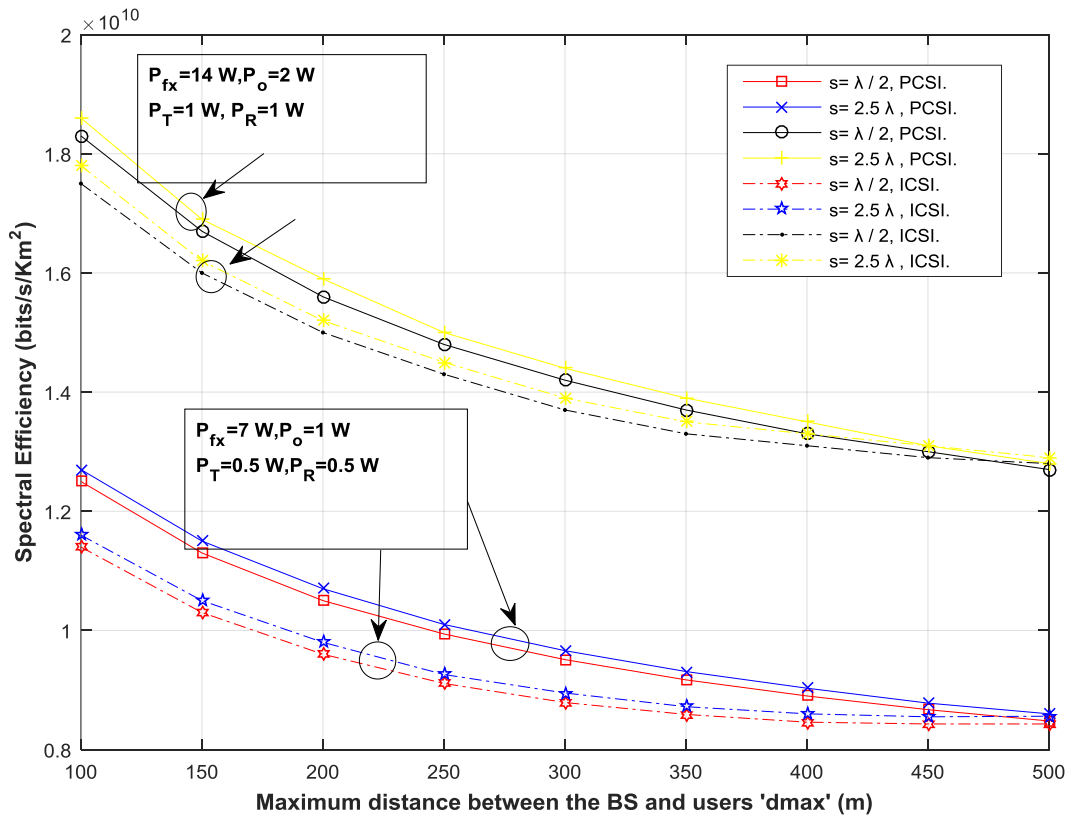


Figure 10. Spectral Efficiency.

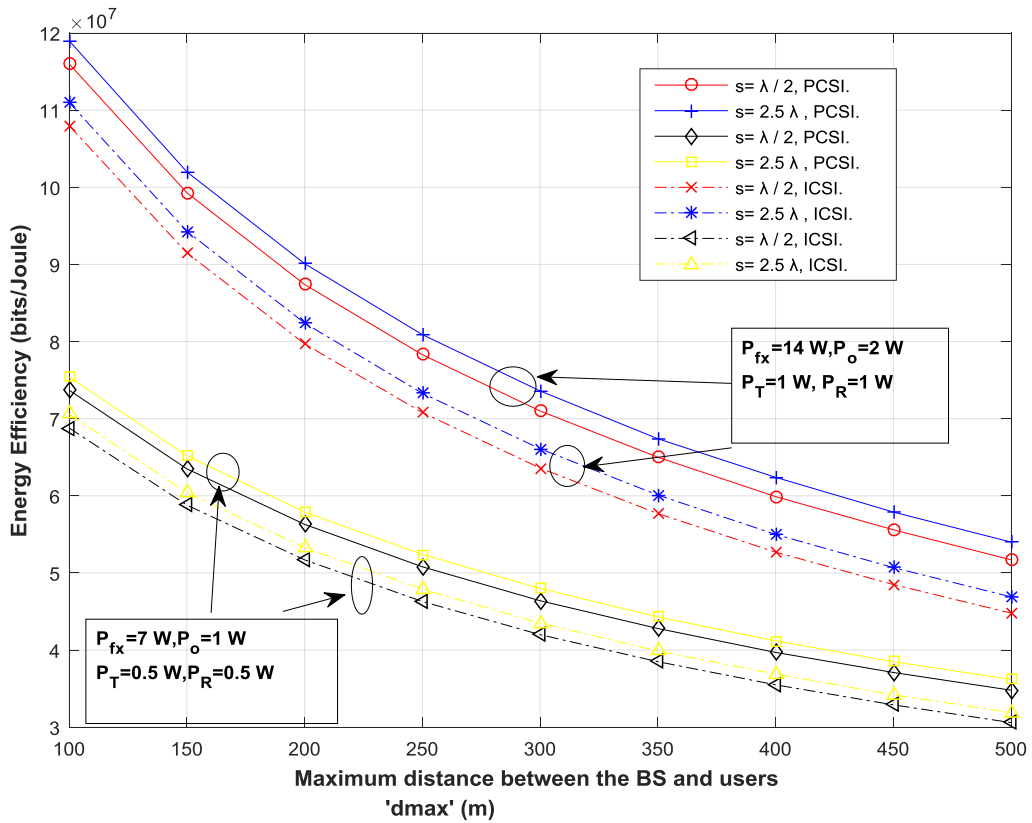


Figure 11. Energy Efficiency.

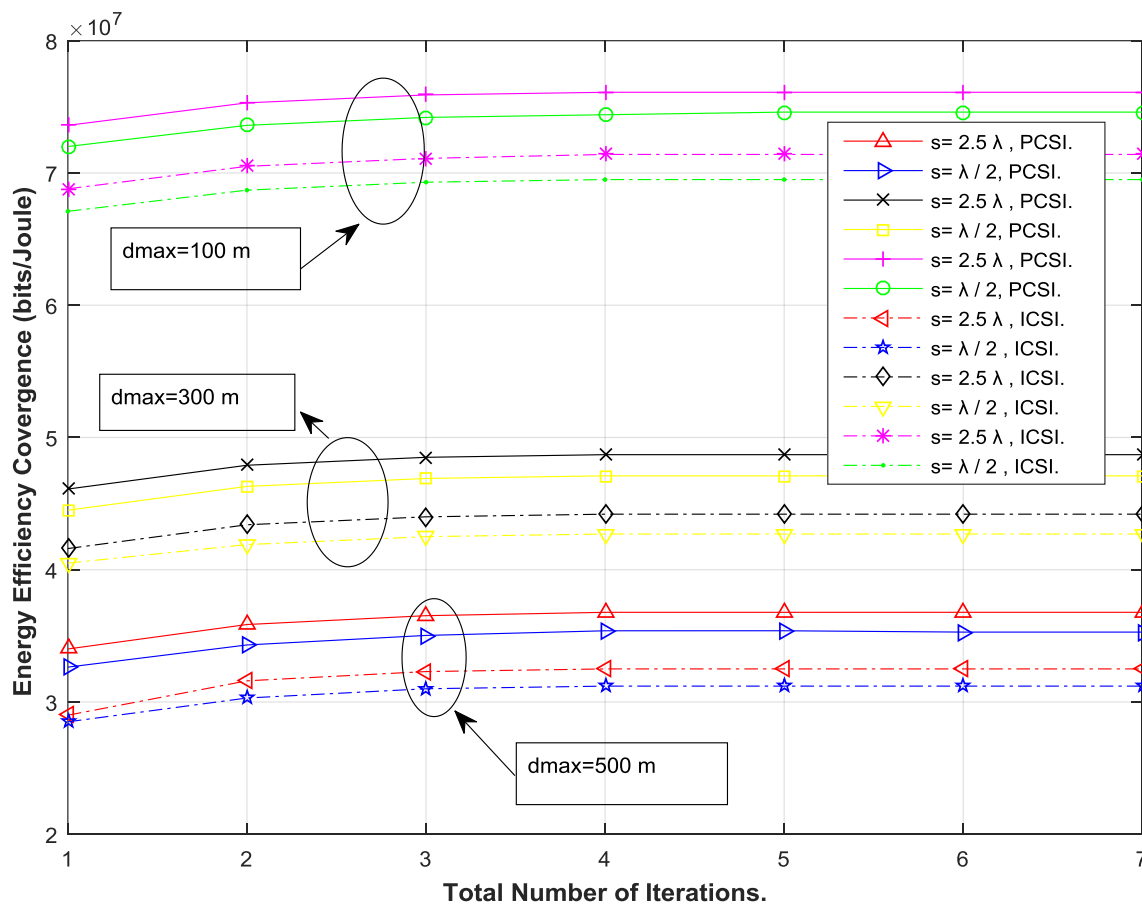


Figure 12. Convergence and the computation Complexity of the domain splitter Algorithm.

7. Conclusions

This article mainly concentrates on the energy efficient designing along with the selection of optimal parameters, with respect to different channel conditions and circuit power consumption levels, by considering the scenario of the urban environment for the Massive MIMO. The energy efficiency and the other optimal system parameters are calculated by using the realistic modelling of the circuit power consumption. The effect of mutual coupling has been deeply investigated on the energy efficiency and other optimal parameters of the system, by varying the length and the inter-distance spacing of the antenna terminals. Closed form expressions of the energy and spectral efficiency are formulated and derived by taking the mutual coupling effect into account. The simulation result shows the mutual coupling effect on the overall optimum energy efficiency and other system parameters. According to the simulation results, we can conclude that it is useful to have the large cell coverage area together with the less power consumption of the circuit. As per the simulation results, the proposed algorithm (domain splitter algorithm) works efficiently without much computational effort. The detailed comparison (Table 2) is presented between the proposed and the reference algorithms. Contrary to the existing researchers, the computation complexity of the proposed domain splitter algorithm is not dependent on the number of the transceiver chains. The mathematical modelling and the simulation results can be so much more beneficial for the future trend of research in order to have the energy efficient communication technologies by controlling the power consumption of the communication devices.

Author Contributions: P.U. perceived the idea and assigned the tasks to the other co-authors. A.A.K. contributed to the formulation of mathematical modelling and derivations and the P.D. worked on the simulations under the

guidance of P.U. M.U. helped on the revising, writing and improving the quality standard of this article. The most useful and the significant contribution goes to the P.U.

Acknowledgments: This research was supported and facilitated by Suranaree University of Technology along with the National Research University Project of Thailand and the Higher Education Research Promotion, Office of the Higher Education Commission. We are grateful to the editor and all the reviews for their crucial and significant comments on this article.

Conflicts of Interest: We declare that there is no conflict of interest associated with this article.

Appendix A

Proof of the Lemma 1: Equation (6) can be written as:

$$R_k = \left[\log_2 \left(1 + \frac{p}{\mathbb{E}(G_k^H G_k)^{-1}} \right) \right]$$

$$R_k = \left[\log_2 \left(1 + \frac{p}{\frac{\mathbb{E}(\text{trace}(H^H H)^{-1})}{K\beta_k \text{trace}(C^H C)}} \right) \right] \quad (\text{A1})$$

For a $m \times m$ Wishart central complex matrix ($W \sim W_m(n, I_n)$) with n degrees of freedom and provided that $n > m$, we get:

$$\mathbb{E}[\text{trace}(W)^{-1}] = \frac{m}{n-m} \quad (\text{A2})$$

By using the identity (A2), (A1) can be simplified as:

$$R_k = \left[\log_2 \left(1 + \frac{p}{\frac{K}{K\beta_k \text{trace}(C^H C)(M-K)}} \right) \right]$$

$$R_k = \left[\log_2 \left(1 + p\beta_k \text{trace}(C^H C) \times (M-K) \right) \right]$$

Appendix B

Proof of the Lemma 2: The mean and variance of the estimated channel \hat{G}_k for the k th user terminal, with the help of MMSE estimator can be expressed as [38]:

$$\hat{G}_k \sim \text{CN} \left(0, \frac{\beta_k}{1 + \frac{1}{KpT^{ul}}} \right)$$

Therefore, the variance of the channel estimation error ε can be written as:

$$\text{var}(\varepsilon) = \text{var}(G) - \text{var}(\hat{G})$$

Thus, the achievable rates of the k th user terminal can be written as:

$$R_k = \log_2 \left(1 + \frac{p / \left(1 + \frac{1}{KpT_p^{ul}} \right)}{\left(\mathbb{E}(G_k^H G_k)^{-1} \times [\text{var}(\varepsilon)]Kp \right) + \mathbb{E}(G_k^H G_k)^{-1}} \right)$$

$$R_k = \log_2 \left(1 + \frac{p / \left(1 + \frac{1}{KpT_p^{ul}} \right)}{\mathbb{E}(G_k^H G_k)^{-1} [(\text{var}(\varepsilon))Kp + 1]} \right) \quad (\text{A3})$$

By using the results of (A1) and (A2), (A3) can be written as:

$$R_k = \log_2 \left(1 + \frac{p / \left(1 + \frac{1}{KpT_p^{ul}} \right)}{\frac{K}{K\beta_k \text{trace}(C^H C)(M-K)} \times \left[\left(1 - \frac{1}{1 + \frac{1}{KpT_p^{ul}}} \right) Kp + 1 \right]} \right)$$

$$R_k = \log_2 \left(1 + \frac{p\beta_k \text{trace}(C^H C) \times (M-K)}{1 + \frac{1}{T_p^{ul}} + \frac{1}{pKT_p^{ul}}} \right)$$

Appendix C

- Calculation of the optimal parameter (r_1) for $EE_P(r_1)$ in terms of r_1 while the remaining dimensions (r_2, r_3) in the interval $[0, v]$ are constant and fixed. The energy efficiency ($EE_P(r_1)$) in terms of r_1 can be written as:

$$EE_P(r_1) = \frac{r_1(v - r_1)d_2}{d_3 + d_4r_1 + d_5r_1^2 + d_6r_1^3}$$

With the following substitutions:

$$d_1 = \beta_k \text{trace}(C^H C), \quad d_2 = \frac{B}{\ln(2)}(1 + d_1r_3(r_2 - 1))$$

$$d_3 = C_0 + \frac{r_3\delta_x B\alpha^2}{\eta}, \quad d_4 = C_1 + r_2D_0, \quad d_5 = C_2 + r_2D_1$$

$$d_6 = C_3 + r_2D_2$$

Differentiate $EE_P(r_1)$ with respect to r_1 in order to calculate the optimal parameter:

$$\frac{d}{dr_1}(EE_P(r_1)) = \frac{d}{dr_1} \left(\frac{r_1(v - r_1)d_2}{d_3 + d_4r_1 + d_5r_1^2 + d_6r_1^3} \right)$$

$$EE'_P(r_1) = \frac{[d_3 + d_4r_1 + d_5r_1^2 + d_6r_1^3] \times \frac{d}{dr_1}(r_1(v - r_1)d_2) - \left[\frac{r_1(v - r_1)d_2}{d_3 + d_4r_1 + d_5r_1^2 + d_6r_1^3} \right] \times \frac{d}{dr_1}(d_3 + d_4r_1 + d_5r_1^2 + d_6r_1^3)}{[d_3 + d_4r_1 + d_5r_1^2 + d_6r_1^3]^2}$$

$$EE'_P(r_1) = \frac{[d_3 + d_4r_1 + d_5r_1^2 + d_6r_1^3][d_2(v - 2r_1)] - [r_1(v - r_1)d_2(d_4 + 2d_5r_1 + 3d_6r_1^2)]}{[d_3 + d_4r_1 + d_5r_1^2 + d_6r_1^3]^2}$$

Equate the above equation to zero in order to get the optimal parameter:

$$EE'_P(r_1) = 0$$

$$[d_3 + d_4r_1 + d_5r_1^2 + d_6r_1^3][(v - 2r_1)] - [r_1(v - r_1)(d_4 + 2d_5r_1 + 3d_6r_1^2)] = 0 \quad (\text{A4})$$

$$\text{At } r_1 = 0; EE'_P(0) = vd_3$$

$$\text{At } r_1 = v; EE'_P(v) = -v[d_3 + d_4r_1 + d_5r_1^2 + d_6r_1^3]$$

Thus, $EE'_P(r_1)$ follows the quasi concave response because $EE'_P(r_1)$ is first positive and then negative with the optimal value must be existed at $EE'_P(r_1) = 0$, and the $EE''_P(r_1)$ must be less than zero:

$$EE''_P(r_1) = \frac{d}{dr_1} \left(\begin{aligned} & [d_3 + d_4r_1 + d_5r_1^2 + d_6r_1^3] \times [(v - 2r_1)] \\ & - [r_1(v - r_1)(d_4 + 2d_5r_1 + 3d_5r_1^2)] \end{aligned} \right)$$

$$EE''_P(r_1) = (v - 2r_1)(d_4 + 2d_5r_1 + 3d_6r_1^2) - 2(d_3 + d_4r_1 + d_5r_1^2 + d_6r_1^3) - [(v - 2r_1)(d_4 + 2d_5r_1 + 3d_6r_1^2) + r_1(v - r_1)(2d_5 + 6d_6r_1)]$$

$$EE''_P(r_1) = - \left[2(d_3 + d_4r_1 + d_5r_1^2 + d_6r_1^3) + r_1(v - r_1)(2d_5 + 6d_6r_1) \right]$$

$$EE''_P(r_1) < 0$$

- Calculation of the optimal parameter (r_2) for $EE_P(r_2)$ in terms of r_2 while the remaining dimensions (r_1, r_3) in the interval $[1, \infty)$ are constant and fixed. Thus, the energy efficiency ($EE_P(r_2)$) in terms of r_2 can be written as:

$$EE_P(r_2) = \frac{d_2 \ln(1 + d_3r_2 - d_3)}{d_4 + d_5r_2}$$

With the following substitutions:

$$d_1 = \beta_k \text{trace}(C^H C), d_2 = r_1 \left(1 - \frac{Tr_1}{U} \right) \frac{B}{\ln(2)},$$

$$d_3 = d_1 r_3, d_4 = \frac{r_3 \delta_x B \alpha^2}{\eta} + \sum_{i=0}^3 C_i r_1^i, d_5 = \sum_{j=0}^2 D_j r_1^{j+1}$$

Differentiate $EE_P(r_2)$ with respect to r_2 to calculate the optimal value:

$$\frac{d}{dr_2} (EE_P(r_2)) = \frac{d}{dr_2} \left(\frac{d_2 \ln(1 + d_3r_2 - d_3)}{d_4 + d_5r_2} \right)$$

$$EE'_P(r_2) = \frac{d_2(d_4 + d_5r_2) \frac{d}{dr_2} (\ln(1 + d_3r_2 - d_3)) - [d_2 \ln(1 + d_3r_2 - d_3) \frac{d}{dr_2} (d_4 + d_5r_2)]}{[d_4 + d_5r_2]^2}$$

$$EE'_P(r_2) = \frac{d_2(d_4 + d_5r_2) \left[\frac{d_3}{1 + d_3r_2 - d_3} \right] - [d_2 \ln(1 + d_3r_2 - d_3) d_5]}{[d_4 + d_5r_2]^2}$$

Equate the above equation to zero to get the optimal value:

$$EE'_P(r_2) = 0$$

$$(d_4 + d_5r_2) \left[\frac{d_3}{1 + d_3r_2 - d_3} \right] - [\ln(1 + d_3r_2 - d_3) d_5] = 0$$

$$d_3(d_4 + d_5r_2) - d_5(1 + d_3r_2 - d_3) \ln(1 + d_3r_2 - d_3) = 0 \tag{A5}$$

At $r_2 = 1$ $EE'_P(1) = d_3[d_4 + d_5]$

At $r_2 = \infty$; $EE'_P(\infty) < 0$

Thus, $EE'_P(r_2)$ follows the quasi concave response because $EE'_P(r_2)$ is first positive and then negative with the optimal value must be existed at $EE'_P(r_2) = 0$, and the $EE''_P(r_2)$ must be less than zero:

$$EE''_P(r_2) = \frac{d}{dr_2} \left((d_4 + d_5r_2) \left[\frac{d_3}{1 + d_3r_2 - d_3} \right] - [\ln(1 + d_3r_2 - d_3) d_5] \right)$$

$$EE_P''(r_2) = d_3d_5 - d_5 \left[\ln(1 + d_3r_2 - d_3) \times d_3 + \frac{(1 + d_3r_2 - d_3)d_3}{1 + d_3r_2 - d_3} \right]$$

$$EE_P''(r_2) = \frac{d_3d_5(1 + d_3r_2 - d_3) - d_3d_5(1 + d_3r_2 - d_3)\ln(1 + d_3r_2 - d_3) - d_3d_5(1 + d_3r_2 - d_3)}{(1 + d_3r_2 - d_3)}$$

$$EE_P''(r_2) = -d_3d_5\ln(1 + d_3r_2 - d_3)$$

$$EE_P''(r_2) < 0$$

- Calculation of the optimal parameter (r_3) for $EE_P(r_3)$ in terms of r_3 while the remaining dimensions (r_1, r_2) in the interval $[1, \infty)$ are constant and fixed. Thus, the energy efficiency ($EE_P(r_3)$) in terms of r_3 can be written as:

$$EE_P(r_3) = \frac{d_2\ln(1 + d_3r_3)}{d_5r_3 + d_4}$$

With the following substitutions:

$$d_1 = \beta_k \text{trace}(C^H C), \quad d_2 = r_1 \left(1 - \frac{Tr_1}{U}\right) \frac{B}{\ln(2)},$$

$$d_3 = d_1(r_2 - 1), \quad d_4 = \sum_{i=0}^3 C_i r_1^i + r_2 \sum_{j=0}^2 D_j r_1^{j+1}, \quad d_5 = \frac{\delta_x B \alpha^2}{\eta}$$

Differentiate $EE_P(r_3)$ with respect to r_3 to calculate the optimal value:

$$\frac{d}{dr_3}(EE_P(r_3)) = \frac{d}{dr_3} \left(\frac{d_2\ln(1 + d_3r_3)}{d_5r_3 + d_4} \right)$$

$$EE_P'(r_3) = \frac{d_2(d_5r_3 + d_4) \frac{d}{dr_3}(\ln(1 + d_3r_3)) - [d_2\ln(1 + d_3r_3) \frac{d}{dr_3}(d_5r_3 + d_4)]}{[d_5r_3 + d_4]^2}$$

$$EE_P'(r_3) = \frac{d_2(d_5r_3 + d_4) \left[\frac{d_3}{1 + d_3r_3} \right] - [d_2\ln(1 + d_3r_3)d_5]}{[d_5r_3 + d_4]^2}$$

Equate the above equation to zero in order to get the optimal value:

$$EE_P'(r_3) = 0$$

$$\frac{d_2(d_5r_3 + d_4) \left[\frac{d_3}{1 + d_3r_3} \right] - [d_2\ln(1 + d_3r_3)d_5]}{[d_5r_3 + d_4]^2} = 0$$

$$d_3(d_5r_3 + d_4) - d_5(1 + d_3r_3)\ln(1 + d_3r_3) = 0 \quad (A6)$$

$$\text{At } r_3 = 1; EE_P'(1) = d_3[d_5 + d_4]$$

$$\text{At } r_3 = \infty; EE_P'(\infty) < 0$$

Thus, $EE_P'(r_3)$ follows the quasi concave response because $EE_P'(r_3)$ is first positive and then negative with the optimal value must be existed at $EE_P'(r_3) = 0$, and the $EE_P''(r_3)$ must be less than zero:

$$EE_P''(r_3) = \frac{d}{dr_3} \left(\frac{d_3(d_5r_3 + d_4)}{-d_5(1 + d_3r_3)\ln(1 + d_3r_3)} \right)$$

$$EE_P''(r_3) = d_3d_5 - d_5 \left[(1 + d_3r_3) \left(\frac{d_3}{1 + d_3r_3} \right) + d_3\ln(1 + d_3r_3) \right]$$

$$EE''_p(r_3) = \frac{d_3 d_5 (1 + d_3 r_3) - d_3 d_5 (1 + d_3 r_3) - d_3 d_5 (1 + d_3 r_3) \ln(1 + d_3 r_3)}{1 + d_3 r_3}$$

$$EE''_p(r_3) = -d_3 d_5 \ln(1 + d_3 r_3)$$

$$EE''_p(r_3) < 0$$

Appendix D

- The optimal parameter (r_1) for $EE_{Im,P}(r_1)$ in terms of r_1 when the other dimensions (r_2, r_3) are fixed can be calculated by using the (A4). Similarly, the optimal parameter (r_2) for $EE_{Im,P}(r_2)$ in terms of r_2 when the other dimensions (r_1, r_3) are fixed can be calculated by using the (A5) but substitute $d_3 = \frac{\beta_k \text{trace}(C^H C)}{1 + \frac{1}{T_p^u} + \frac{1}{r_3 T_p^u}} \times r_3$ in the (A5).
- Calculation of the optimal parameter (r_3) for $EE_{Im,P}(r_3)$ in terms of r_3 while the remaining dimensions (r_1, r_2) in the interval $[1, \infty)$ are constant and fixed. Thus, the energy efficiency ($EE_{Im,P}(r_3)$) in terms of r_3 can be written as:

$$EE_{Im,P}(r_3) = \frac{d_1 \ln \left(1 + \frac{d_2 r_3}{d_6 + \frac{d_3}{r_3}} \right)}{d_4 r_3 + d_5}$$

With the following substitutions:

$$d_1 = r_1 \left(1 - \frac{Tr_1}{U} \right) \frac{B}{\ln(2)}, \quad d_2 = (r_2 - 1) \beta_k \text{trace}(C^H C), \quad d_3 = \frac{1}{T_p^u},$$

$$d_4 = \frac{\delta_x B a^2}{\eta}, \quad d_5 = \sum_{i=0}^3 C_i r_1^i + r_2 \sum_{j=0}^2 D_j r_1^{j+1}, \quad d_6 = 1 + d_3$$

Differentiate $EE_{Im,P}(r_3)$ with respect to r_3 in order to calculate the optimal parameter:

$$\frac{d}{dr_3} (EE_{Im,P}(r_3)) = \frac{d}{dr_3} \left(\frac{d_1 \ln \left(1 + \frac{d_2 r_3}{d_6 + \frac{d_3}{r_3}} \right)}{d_4 r_3 + d_5} \right)$$

$$EE'_{Im,P}(r_3) = \frac{d_1 (d_4 r_3 + d_5) \frac{d}{dr_3} \left(\ln \left(1 + \frac{d_2 r_3}{d_6 + \frac{d_3}{r_3}} \right) \right) - d_1 \ln \left(1 + \frac{d_2 r_3}{d_6 + \frac{d_3}{r_3}} \right) \frac{d}{dr_3} (d_4 r_3 + d_5)}{(d_4 r_3 + d_5)^2}$$

$$EE'_{Im,P}(r_3) = \frac{d_1 (d_4 r_3 + d_5) \frac{d}{dr_3} \left(\ln \left(1 + \frac{d_2 r_3}{d_6 + \frac{d_3}{r_3}} \right) \right) - d_1 d_4 \ln \left(1 + \frac{d_2 r_3}{d_6 + \frac{d_3}{r_3}} \right)}{(d_4 r_3 + d_5)^2} \quad (A7)$$

where

$$\frac{d}{dr_3} \left(\ln \left(1 + \frac{d_2 r_3}{d_6 + \frac{d_3}{r_3}} \right) \right) = \frac{1}{1 + \frac{d_2 r_3}{d_6 + \frac{d_3}{r_3}}} \times \frac{\left(d_6 + \frac{d_3}{r_3} \right) d_2 - d_2 r_3 \left(-r_3 x_3^{-2} \right)}{\left(d_6 + \frac{d_3}{r_3} \right)^2}$$

$$\frac{d}{dr_3} \left(\ln \left(1 + \frac{d_2 r_3}{d_6 + \frac{d_3}{r_3}} \right) \right) = \frac{1}{\frac{d_6 + d_3 r_3^{-1} + d_2 r_3}{d_6 + d_3 r_3^{-1}}} \times \frac{\left(d_6 + \frac{d_3}{r_3} \right) d_2 - d_2 r_3 \left(-r_3 x_3^{-2} \right)}{\left(d_6 + \frac{d_3}{r_3} \right)^2}$$

$$\frac{d}{dr_3} \left(\ln \left(1 + \frac{d_2 r_3}{d_6 + \frac{d_3}{r_3}} \right) \right) = \frac{d_2 \left[1 + \frac{d_3}{d_6 r_3 + d_3} \right]}{d_6 + d_2 r_3 + d_3 r_3^{-1}}$$

Therefore, the (A7) can be written as:

$$EE'_{Im,P}(r_3) = \frac{d_1(d_4 r_3 + d_5) \frac{d_2 \left[1 + \frac{d_3}{d_6 r_3 + d_3} \right]}{d_6 + d_2 r_3 + d_3 r_3^{-1}} - d_1 d_4 \ln \left(1 + \frac{d_2 r_3}{d_6 + \frac{d_3}{r_3}} \right)}{(d_4 r_3 + d_5)^2}$$

Equate the above equation to zero in order to get the optimal parameter:

$$EE'_{Im,P}(r_3) = 0$$

$$(d_4 r_3 + d_5) \frac{d_2 \left[1 + \frac{d_3}{d_6 r_3 + d_3} \right]}{d_6 + d_2 r_3 + d_3 r_3^{-1}} - d_4 \ln \left(1 + \frac{d_2 r_3}{d_6 + \frac{d_3}{r_3}} \right) = 0$$

$$d_2(d_4 r_3 + d_5) \left[1 + \frac{d_3}{d_6 r_3 + d_3} \right] - d_4 (d_6 + d_2 r_3 + d_3 r_3^{-1}) \ln \left(1 + \frac{d_2 r_3}{d_6 + \frac{d_3}{r_3}} \right) = 0 \quad (A8)$$

$$\text{At } r_3 = 1; EE'_{Im,P}(1) = d_2(d_4 r_3 + d_5) \left[1 + \frac{d_3}{d_6 r_3 + d_3} \right]$$

$$\text{At } r_3 = \infty; EE'_{Im,P}(\infty) < 0$$

$$EE'_{Im,P}(1) = d_2(d_4 r_3 + d_5) \left[1 + \frac{d_3}{d_6 r_3 + d_3} \right]$$

$$EE'_{Im,P}(\infty) < 0$$

Thus, $EE'_{Im,P}(r_3)$ follows the quasi concave response because $EE'_{Im,P}(r_3)$ is first positive and then negative with the optimal value must be existed at $EE'_{Im,P}(r_3) = 0$, and the $EE''_{Im,P}(r_3)$ must be less than zero:

$$EE''_{Im,P}(r_3) = \frac{d}{dr_3} \left(d_2(d_4 r_3 + d_5) \left[1 + \frac{d_3}{d_6 r_3 + d_3} \right] - d_4 (d_6 + d_2 r_3 + d_3 r_3^{-1}) \times \ln \left(1 + \frac{d_2 r_3}{d_6 + \frac{d_3}{r_3}} \right) \right)$$

$$EE''_{Im,P}(r_3) = d_2(d_4 r_3 + d_5) \left[\frac{-d_3 d_6}{(d_3 + d_6 r_3)^2} \right] + d_4 d_2 \left[1 + \frac{d_3}{d_3 + d_6 r_3} \right] - d_4 \left[d_2 \left(1 + \frac{d_3}{d_6 r_3 + d_3} \right) + \left(d_2 - \frac{d_3}{r_3^2} \right) \right]$$

$$EE''_{Im,P}(r_3) = - \left[\frac{d_2 d_3 d_6 (d_4 r_3 + d_5)}{(d_3 + d_6 r_3)^2} + \left(\frac{d_4 d_2 r_3^2 - d_3 d_4}{r_3^2} \right) \times \ln \left(1 + \frac{d_2 r_3}{d_6 + \frac{d_3}{r_3}} \right) \right]$$

$$EE''_{Im,P}(r_3) < 0$$

References

1. Vu, T.X.; Chatzinotas, S.; Ottersten, B. Edge-caching wireless networks: Energy-efficient design and optimization. *IEEE Trans. Wirel. Commun.* **2018**, *17*, 2827–2839. [CrossRef]
2. Ramezani, P.; Jamalipour, A. Toward the evolution of wireless powered communication networks for the future Internet of Things. *IEEE Netw.* **2017**, *31*, 62–69. [CrossRef]
3. Cisco. *Cisco Visual Networking Index: Global Mobile Data Traffic Forecast Update 2016–2021*; White Paper; Cisco: San Jose, CA, USA, 2017.

4. Ma, S.; Yang, Y.; Sharif, H. Distributed MIMO technologies in cooperative wireless networks. *IEEE Commun. Mag.* **2011**, *49*, 78–82. [[CrossRef](#)]
5. Marzetta, T.L. Noncooperative cellular wireless with unlimited numbers of base station antennas. *IEEE Trans. Wirel. Commun.* **2010**, *9*, 3590–3600. [[CrossRef](#)]
6. Rusek, F.; Persson, D.; Lau, B.K.; Larsson, E.G.; Marzetta, T.L.; Edfors, O.; Tufvesson, F. Scaling up MIMO: Opportunities and challenges with very large arrays. *IEEE Signal Process. Mag.* **2013**, *30*, 40–46. [[CrossRef](#)]
7. Kamga, G.N.; Xia, M.; Aissa, S. Spectral-Efficiency Analysis of Regular- and Large-Scale (Massive) MIMO with a Comprehensive Channel Model. *IEEE Trans. Veh. Technol.* **2017**, *66*, 4984–4996. [[CrossRef](#)]
8. Andrews, J.G.; Buzzi, S.; Choi, W.; Hanly, S.V.; Lozano, A.; Soong, A.C.K.; Zhang, J.C. What will 5G be? *IEEE J. Sel. Areas Commun.* **2014**, *32*, 1065–1082. [[CrossRef](#)]
9. Björnson, E.; Larsson, E.G.; Marzetta, T.L. Massive MIMO: Ten myths and one critical question. *IEEE Commun. Mag.* **2016**, *54*, 114–123. [[CrossRef](#)]
10. Lu, L.; Li, G.Y.; Swindlehurst, A.L.; Ashikhmin, A.; Zhang, R. An overview of massive MIMO: Benefits and challenges. *IEEE J. Sel. Top. Signal Process.* **2014**, *8*, 742–758. [[CrossRef](#)]
11. Wang, Z.; Simeoni, M.; Lager, I.E. A complete tool for Analyzing Mutual Couplings in Nonuniform Arrays of Rectangular Aperature Radiators. *IEEE Antennas Wirel. Prog. Mag.* **2017**, *16*, 3192–3195. [[CrossRef](#)]
12. Wallace, J.W.; Jensen, M.A. Mutual coupling in MIMO wireless systems: A rigorous network theory analysis. *IEEE J. Select. Areas Commun.* **2004**, *3*, 1317–1325. [[CrossRef](#)]
13. Clerckx, B.; Craeye, C.; Vanhoenacker-Janvier, D.; Oestges, C. Impact of antenna coupling on 2×2 MIMO communications. *IEEE Trans. Veh. Technol.* **2007**, *56*, 1009–1018. [[CrossRef](#)]
14. Boccardi, F.; Heath, R.W.; Lozano, A.; Marzetta, T.L.; Popovski, P. Five disruptive technology directions for 5G. *IEEE Commun. Mag.* **2014**, *52*, 74–80. [[CrossRef](#)]
15. Artiga, X.; Devillers, B.; Perruisseau-Carrier, J. Mutual coupling effects in multi-user massive MIMO base stations. In Proceedings of the 2012 International Symposium on Antennas Propagation, Chicago, IL, USA, 8–14 July 2012; pp. 1–2.
16. Ge, X.; Zi, R.; Wang, H.; Zhang, J.; Jo, M. Multi-user massive MIMO communication systems based on irregular antenna arrays. *IEEE Trans. Wirel. Commun.* **2016**, *15*, 5287–5301. [[CrossRef](#)]
17. Nishimori, K.; Hiraguri, T.; Ogawa, T.; Yamada, H. Throughput performance on IEEE802. 11ac based massive MIMO considering calibration errors. In Proceedings of the International Symposium on Antennas Propagation, Kaohsiung, Taiwan, 2–5 December 2014; pp. 395–396.
18. Nishimori, K.; Hiraguri, T.; Ogawa, T.; Yamada, H. Effectiveness Of implicit beamforming using calibration technique in massive MIMO System. In Proceedings of the 2014 IEEE International Workshop Electromagnetics, Sapporo, Japan, 4–6 August 2014; pp. 117–118.
19. Wei, H.; Wang, D.; Zhu, H.; Wang, J.; Sun, S.; You, X.H. Mutual coupling calibration for multiuser massive MIMO systems. *IEEE Trans. Wirel. Commun.* **2016**, *15*, 606–619. [[CrossRef](#)]
20. Shirazinia, A.; Dey, S.; Ciuonzo, D.; Rossi, P.S. Massive MIMO for Decentralized Estimation of a Correlated Source. *IEEE Trans. Signal Process.* **2016**, *64*, 2499–2512. [[CrossRef](#)]
21. Ciuonzo, D.; Rossi, P.S.; Dey, S. Massive MIMO meets decision fusion: Decode-and-fuse vs. decode-then-fuse. In Proceedings of the 2014 IEEE 8th Sensor Array and Multichannel Signal Processing Workshop (SAM), A Coruna, Spain, 22–25 June 2014.
22. Tombaz, S.; Vastberg, A.; Zander, J. Energy- and cost-efficient ultrahigh-capacity wireless access. *IEEE Wirel. Commun. Mag.* **2011**, *18*, 18–24. [[CrossRef](#)]
23. Zhang, D.; Tariq, M.; Mumtaz, S.; Rodriguez, J.; Sato, T. Integrating energy efficiency analysis of massive MIMO-based C-RAN. *EURASIP J. Wirel. Commun. Netw.* **2016**, *1*, 277–286. [[CrossRef](#)]
24. Xiao, X.; Tao, X.; Lu, J. Energy-efficient resource allocation in LTE based MIMO-OFDMA systems with user rate constraints. *IEEE Trans. Veh. Technol.* **2015**, *64*, 185–197. [[CrossRef](#)]
25. Tsinos, C.G.; Maleki, S.; Chatzinotas, S.; Ottersten, B. On the Energy-Efficiency of Hybrid Analog-Digital Transceivers for Single- and Multi-Carrier Large Antenna Array Systems. In Proceedings of the IEEE International Conference on Communications 579 (ICC), Paris, France, 21–25 May 2017.
26. Garcia-Rodriguez, A.; Venkateswaran, V.; Rulikowski, P.; Masouros, C. Hybrid Analog–Digital Precoding Revisited Under Realistic RF Modeling. *IEEE Wirel. Commun. Lett.* **2016**, *5*, 528–531. [[CrossRef](#)]

27. Tsinos, C.G.; Maleki, S.; Chatzinotas, S.; Ottersten, B. On the Energy-Efficiency of Hybrid Analog-Digital Transceivers for Single- and Multi-Carrier Large Antenna Array Systems. *IEEE J. Sel. Areas Commun.* **2017**, *35*, 1980–1995. [[CrossRef](#)]
28. Ngo, H.; Larsson, E.; Marzetta, T. Energy and spectral efficiency of very large multiuser MIMO systems. *IEEE Trans. Commun.* **2013**, *61*, 1436–1449.
29. Bjornson, E.; Hoydis, J.; Kountouris, M.; Debbah, M. Massive MIMO systems with non-ideal hardware: Energy efficiency, estimation, and capacity limits. *IEEE Trans. Inf. Theory.* **2014**, *60*, 7112–7139. [[CrossRef](#)]
30. Ha, D.; Lee, K.; Kang, J. Energy efficiency analysis with circuit power consumption in massive MIMO systems. In Proceedings of the IEEE International Symposium Personal, Indoor and Mobile Radio Commun. (PIMRC), London, UK, 8–11 September 2013.
31. Yang, H.; Marzetta, T. Total energy efficiency of cellular large scale antenna system multiple access mobile networks. In Proceedings of the IEEE Online Conference on Green Communications (OnlineGreenComm), Piscataway, NJ, USA, 29–31 October 2013.
32. Björnson, E.; Sanguinetti, L.; Hoydis, J.; Debbah, M. Optimal design of energy-efficient multi-user MIMO systems: Is massive MIMO the answer? *IEEE Trans. Wirel. Commun.* **2015**, *14*, 3059–3075. [[CrossRef](#)]
33. Xu, W.; Li, S.; Wang, S.; Feng, Z.; Lin, J.; Vasilakos, A.V. Joint parameter selection for massive MIMO: An energy-efficient perspective. *IEEE Access* **2016**, *4*, 3719–3731. [[CrossRef](#)]
34. Khan, A.A.; Uthansakul, P.; Uthansakul, M. Energy Efficient Design of Massive MIMO by Incorporating with Mutual Coupling. *Int. J. Comm. Antenna Prop.* **2017**, *7*, 198–207. [[CrossRef](#)]
35. Balanis, C.A. *Antenna Theory: Analysis and Design*; John Wiley and Sons: Hoboken, NJ, USA, 2012.
36. Khan, A.A.; Uthansakul, P.; Duangmanee, P.; Uthansakul, M. Energy Efficient Design of Massive MIMO by Considering the Effects of Nonlinear Amplifiers. *Energies* **2018**, *11*, 1045. [[CrossRef](#)]
37. Biswas, S.; Masouros, C.; Ratnarajah, T. On the energy efficiency of massive MIMO with space-constrained 2D antenna arrays. In Proceedings of the IEEE International Conference on Communications, Kuala Lumpur, Malaysia, 22–27 May 2016.
38. Ciunzo, D.; Rossi, P.S.; Dey, S. Massive MIMO channel-aware decision fusion. *IEEE Trans. Signal Process.* **2015**, *63*, 604–619. [[CrossRef](#)]



© 2018 by the authors. Licensee MDPI, Basel, Switzerland. This article is an open access article distributed under the terms and conditions of the Creative Commons Attribution (CC BY) license (<http://creativecommons.org/licenses/by/4.0/>).